in the precipitates from the experiment of pH range from 6.00 to 9.00 indicates that some of the crystal cells of the precipitate have been in equilibrium with a different pH before reaching the final pH of solution, since cell expansion process takes a certain amount of time.

As a conclusion, X-ray diffraction pattern for the precipitate in uranyl hydrolysis reaction was strongly dependent on the pH values, where their precipitates were formed as well as where the precipitates are in equilibrium with. A layered structure of the precipitates became amorphous when the precipitate were formed at pH >9.7. Greater solubility for the precipitate formed at higher pH value can be explained from the fact that the precipitates formed at lower pH value had a better crystallinity and also that the precipitates formed at higher pH value has a slower rate of crystallization. The thickness of the unit layer of UHPs increases with the pH values at which the precipitate was synthesized as well as the pH values of the solution.

References

1. Wang, R. *Spent Fuel Special Studies Progress Report: Probable Mechanisms for Oxidation and Dissolution of Single-Crystal UO_2 surfaces*, PNL-3566, Pacific Northwest Laboratory, Richland, Washington, 1981.
2. Vandergraaf, T. T. *Leaching of Irradiated UO_2* Fuel, Technical Record TR-100, Whiteshell Nuclear Research Establishment, Pinawa, Manitoba, Canada, 1980.
3. Bruno, J.; Casas, I.; Lagerman, B.; Munoz, M. *Mat. Res. Soc. Symp. Proc.* **1987**, *84*, 153.
4. Nitsche, H. *Radiochimica Acta* **1991**, *52/53*, 3.
5. Christ, C. L.; Clark, J. R. *Am. Mineral.* **1960**, *45*, 1026.
6. *Joint Commitee on Powder Diffractio Standards, Powder Diffraction File Sets* 11-15 (revised), p 480.

Redox Chemistry and Autoreduction of Non-μ-oxo Dimer-Forming [5,10,15,20-Tetrakis(2,6-dichlorophenyl)porphyrinato] Manganese(III) Chloride by Hydroxide Ion

Seungwon Jeon*, Hyo Kyoung Lee, and Yong-Kook Choi

Department of Chemistry, Chonnam National University, Kwang-ju 500-757, Korea

Received June 26, 1996

The electrochemistry and the reaction of non-μ-oxo dimer-forming [5,10,15,20-tetrakis(2,6-dichlorophenyl)porphyrinato] manganese(III) chloride [$(Cl_8TPP)Mn^{III}Cl$] with tetraethylammonium hydroxide in water [$OH(H_2O)$] have been investigated by electrochemical and spectroscopic methods under anaerobic conditions. The stronger autoreduction of $(Cl_8TPP)Mn^{III}Cl$ by $^-OH(H_2O)$ in comparison with $(Me_{12}TPP)Mn^{III}Cl$ by $^-OH(CH_3OH)$ in MeCN is explained as the influence of electronic effects on substituted phenyl groups bonded to *meso*-position of porphyrin ring and the positive shift of reduction potential (−0.11 V) for $(C_{18}TPP)Mn^{III}Cl$. The autoreduction of manganese(III) porphyrin to manganese (II) by this process is only observed when one axial position is occupied by a ligating solvent and OH coordinates the other axial site. The results are discussed in relation to the mechanisms for the reduction of manganese(III) porphyrin.

Introduction

Metalloporphyrins can experience reversible redox reactions in which the site of electron transfer may be localized at either the central metal or the porphyrin ring. Manganese porphyrins have several interesting aspects of physical, chemical, and biological properties which distinguish them from other metalloporphyrins.[1~3] Manganese porphyrins continue to be of interest as models for the behavior of cytochrome P-450,[4~5] photosystem II,[6~7] and superoxide dismutase,[8] as DNA binding and cleavage reagents,[9~11] and as catalysts for the epoxidation of olefins.[12~16] Axial ligation of manganese porphyrins coupled with redox chemistry is very important in diverse biological functions.[17~22]

Electrochemical studies on the redox properties of manganese porphyrins are numerous.[23~27] Manganese porphyrins have been studied by electrochemical methods in the fields of electron transfer kinetics and ligand addition reactions,[28~29] counterion and solvent effects,[30~31] and porphyrin substituent effects.[32]

A kind of metalloenzyme containing manganese as a core metal mediates the oxidation of water to dioxygen in green plant photosynthesis by variations in its oxidation and ligation states.[33~34] The oxidation of water to produce dioxygen is presumably less understood. It was recently reported that the reaction of manganese(III) tetramesitylporphyrin with excess methanolic hydroxide ion [$OH(CH_3OH)$] in ligating and nonligating solvents resulted in the formation of manganese(II) which in a slower reaction is oxidized to manganese (III).[35~36] The mechanism for the oxidation of manganese(II) to manganese(III) is still ambiguous. In that report, because methanolic hydroxide ion is used, manganese(II) can be oxi-

dized by methoxide ion generated from the methanolic hydroxide ion.

In the present study, in order to exclude the existence of methoxide ion, tetraethylammonium hydroxide in water [TEAOH(in H_2O)] is used as a source of hydroxide ion. We investigate the redox chemistry and the stoichiometric reactions of non-μ-oxo dimer-forming [5,10,15,20-tetrakis(2,6-dichlorophenyl)porphyrinato] manganese(III) chloride [(Cl_8TPP)$Mn^{III}Cl$] with TEAOH (in H_2O) in ligating and nonligating solvents. We describe the stronger autoreduction of (Cl_8TPP)$Mn^{III}Cl$ by $OH(H_2O)$ in comparison with (Me_{12}TPP)$Mn^{III}Cl$ by $OH(CH_3OH)$ in MeCN, this result will be explained as the influence of electronic effects on substituted phenyl groups bonded to *meso*-position of porphyrin ring. The electrochemical and spectroscopic results will be discussed in view of the factors for the determining the autoreduction pathway.

Experimental

Materials. 5,10,15,20-tetrakis(2,6-dichlorophenyl)porphyrin [(Cl_8TPP)H_2] was synthesized by the method of Lindsey *et al.* and manganese [(Cl_8TPP)$Mn^{III}Cl$] was inserted by the standard route.[37-38] (Cl_8TPP)$Mn^{III}ClO_4$ was prepared by the reaction of (Cl_8TPP)$Mn^{III}Cl$ with anhydrous $AgClO_4$ in hot toluene.[20] Anhydrous acetonitrile, methylene chloride, and other solvents (Aldrich) were used as received from the supplier. Tetraethylammonium hydroxide (TEAOH) [Et_4NOH, Aldrich, 20 wt.% in water [$OH(H_2O)$]] was used as received. Samples of (Cl_8TPP)Mn^{II} were prepared by the electrochemical reduction of (Cl_8TPP)$Mn^{III}Cl$ or by the reduction of (Cl_8TPP)$Mn^{III}Cl$ with amalgamated zinc in toluene in a Vacuum Atmospheres glove box. (Cl_8TPP)$Mn^{III}OH$ was prepared by established procedure.[14] Tetrabuthyl-ammonium perchlorate (Bu_4NClO_4) was used as a supporting electrolyte.

Instrumentation and Methodology. The cyclic voltammetric measurements were accomplished with a three-electrode potentiostat (Bioanalytical Systems, Model CV-27) and a Linseis Model LY 18100 recorder. A platinum-wire electrode separated from the analyte compartment by a medium porosity glass frit was used as the auxiliary electrode. A Ag/AgCl electrode supplied by BAS was used as the reference electrode, and the potential is approximately −45 mV relative to a saturated calomel electrode (SCE). A 3.0 mm diameter glassy carbon was employed as the working electrode for the redox reactions of manganese porphyrins. All working electrode surfaces were highly polished with Al_2O_3 paste prior to each experiment. The reproducibility of individual potential values was ± 5 mV. The various oxidation states of manganese were electrochemically generated via controlled-potential electrolysis using CV-27 potentiostat with a three electrode system in a 1-mm quartz cuvette containing a Pt mesh working electrode. Absorption spectra were recorded on a Hewlett Packard 8452A Diode Array spectrophotometer interfaced to a computer. The reaction solutions of (Cl_8TPP)$Mn^{III}Cl$ with $OH(H_2O)$ were prepared under an argon atmosphere and placed in a UV-vis cuvette with rubber septum and sealed with parafilm.

Results

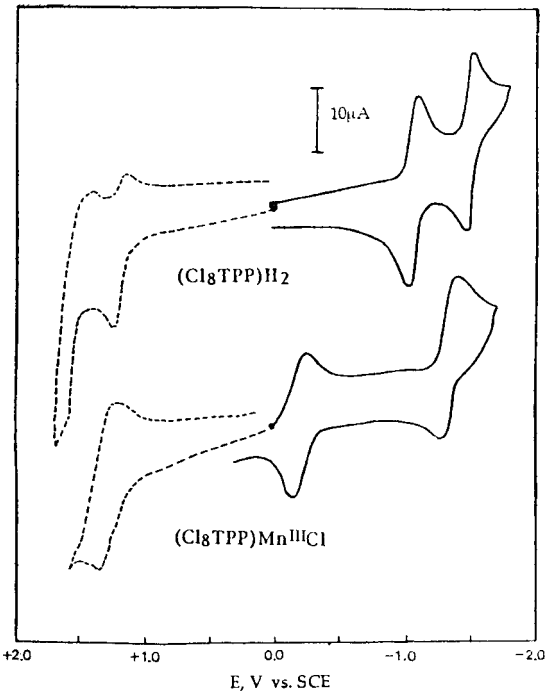

Figure 1. Cyclic voltammograms in MeCN (0.1 M Bu_4NClO_4) of (top) 1.0 mM (Cl_8TPP)H_2 and (bottom) 1.0 mM (Cl_8TPP)$Mn^{III}Cl$ at a glassy carbon electrode (scan rate, 0.1 Vs^{-1}). The oxidations of (Cl_8TPP)H_2 and (Cl_8TPP)$Mn^{III}Cl$ (dot line), the reductions of (Cl_8TPP)H_2 and (Cl_8TPP)$Mn^{III}Cl$ (solid line).

Electrochemical and Spectroelectrochemical studies for Manganese Tetra(2,6-dichlorophenyl)porphyrins. Figure 1 illustrates the cyclic voltammograms for (Cl_8TPP)H_2 and (Cl_8TPP)$Mn^{III}Cl$ at a glassy carbon electrode in MeCN (0.1 M Bu_4NClO_4). The formal potentials ($E^{\circ\prime}$) for manganese porphyrins are summarized in Table 1. The oxidation and reduction of manganese porphyrins is well established to be either metal or ligand centered. The first oxidation potential (+1.46 V *vs.* SCE) for (Cl_8TPP)$Mn^{III}Cl$ in Table 1 is slightly positive of those for (Me_{12}TPP)$Mn^{III}Cl$ and (TPP)$Mn^{III}ClO_4$. The first oxidation of (Cl_8TPP)$Mn^{III}Cl$ (λ_{max} = 476 nm) in MeCN gives a manganese(III) porphyrin π-cation radical ($Cl_8TPP^{\cdot}$)$Mn^{III}Cl$ (λ_{max} = 388 nm, 487 nm) by one-electron transfer with ligand centered which is consistent with previous reports.[35] Unfortunately the second oxidation potential for (Cl_8TPP)$Mn^{III}Cl$ couldn't be measured in MeCN, but it should be slightly positive of those for (Me_{12}TPP)$Mn^{III}Cl$ and (TPP)$Mn^{III}ClO_4$. The more positive potential for the oxidation of (Cl_8TPP)$Mn^{III}Cl$ comes from the electronic effects of the substituted groups at *ortho*-position of phenyl group bonded to *meso*-position of porphyrin ring.

While the first oxidation potential for (Cl_8TPP)$Mn^{III}OH$ (see Figure 2), which exchanges chloride ion in (Cl_8TPP)$Mn^{III}Cl$ for hydroxide ion, changes to +1.21 V from +1.46 V for (Cl_8TPP)$Mn^{III}Cl$. The oxidation product of (Cl_8TPP)$Mn^{III}OH$ seems to be (Cl_8TPP)$Mn^{IV}(O)$ or (Cl_8TPP)$Mn^{IV}(OH)_2$ by one-electron transfer with metal centered rather than ligand centered. The species (Cl_8TPP)$Mn^{IV}(O)$ or (Cl_8TPP)$Mn^{IV}(OH)_2$ shows a Soret absorbance at 425 nm which is consistent with previous results on manganese(IV) porphyrins.[14]

Table 1. Voltammetric Redox Potentials for Manganese Porphyrins in MeCN [0.1 M $(Bu_4N)ClO_4$]

Substrate	$E^{1/2}$ (V *vs* SCE)					
(S)	$(P^{2+})Mn^{III}/(P^{\cdot+})Mn^{III}$	$(P^{\cdot+})Mn^{III}/(P)Mn^{III}$	$(P)Mn^{III}/(P)Mn^{II}$	$(P)Mn^{II}/(P^{\cdot-})Mn^{III}$	$(P^{\cdot-})Mn^{II}/(P^{2-})Mn^{II}$	ref[a]
$(TPP)Mn^{III}Cl$	–	–	−0.23	−1.47	–	1
$(TPP)Mn^{III}ClO_4$	+1.51	+1.25	−0.19	–	–	1
$(Me_{12}TPP)Mn^{III}Cl$	+1.40	+1.11	−0.30	−1.52	−1.98	2
$(Cl_8TPP)Mn^{III}Cl$	–	+1.46	−0.11	−1.34	−1.70	w
$(Cl_8TPP)Mn^{III}ClO_4$	–	+1.49	−0.08	−1.33	−1.68	w

[a] Indicates that 1: ref. 30. 2: ref. 35, w: this work

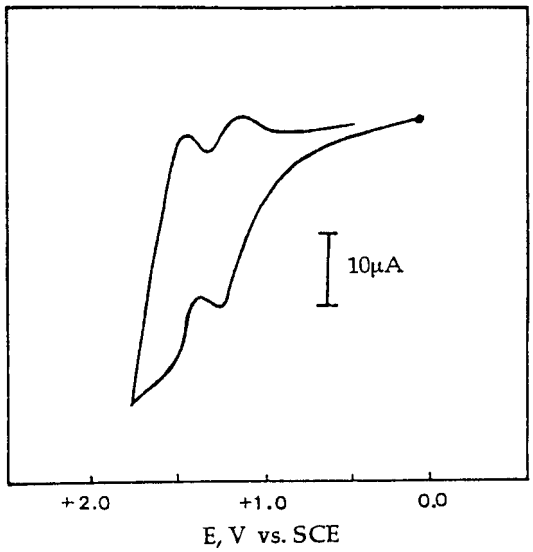

Figure 2. Cyclic voltammogram in CH_2Cl_2 (0.1 M Bu_4NClO_4) of 1.0 mM $(Cl_8TPP)Mn^{III}OH$ at a glassy carbon electrode (scan rate, 0.1 Vs^{-1}).

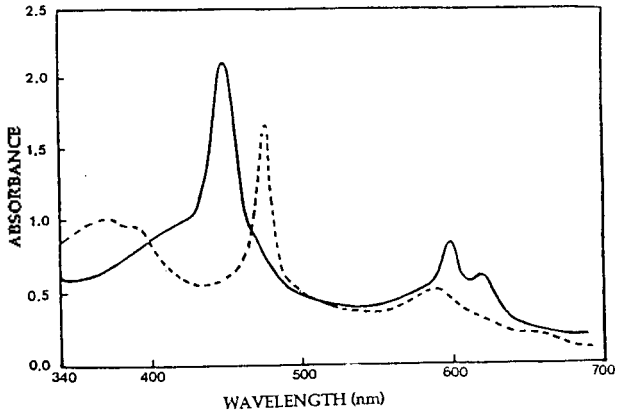

Figure 3. UV-vis absorption spectra of an MeCN solution of (dot line) $(Cl_8TPP)Mn^{III}Cl$ (0.02 mM) and (solid line) product formed by the reaction $(Cl_8TPP)Mn^{III}Cl$ with excess $OH(H_2O)$ under an argon atmosphere.

The UV-visible spectra of $(Cl_8TPP)Mn^{III}OH$ and the products of its first and second oxidation in CH_2Cl_2 are similar to those of $(Me_{12}TPP)Mn^{III}OH$.[35~36] The second oxidation of $(Cl_8TPP)Mn^{III}OH$ {the first oxidation of $(Cl_8TPP)Mn^{IV}(O)$ (+1.42 V in CH_2Cl_2) produces a spectrum with a Soret absorbance at 420 nm by the controlled-potential oxidation. The spectrum is typical of manganese(V) species which exhibits characteristic Soret position, and the product of its second oxidation may be $(Cl_8TPP)Mn^{V}(O)(Cl)$ by one-electron transfer with metal centered.

It was well known that manganese(III) porphyrins undergo three-step one-electron reductions. The results for the electrochemical reduction of manganese porphyrins are also shown in Figure 1 and Table 1. The first reduction potential (−0.11 V *vs.* SCE) for $(Cl_8TPP)Mn^{III}Cl$ is also slightly positive of those for $(Me_{12}TPP)Mn^{III}Cl$ and $(TPP)Mn^{III}ClO_4$. The controlled-potential reduction of $(Cl_8TPP)Mn^{III}Cl$ with optically transparent thin-layer electrode gives the visible spectrum of lower valent states. The first one-electron reduction (−0.11 V) yields $(Cl_8TPP)Mn^{II}$ in MeCN, and the second reduction (−1.34 V) of $(Cl_8TPP)Mn^{III}Cl$ provides a UV-vis spectrum assigned to the anion-radical porphyrin of manganese $(Cl_8TPP^{\cdot-})Mn^{II}$. $(Cl_8TPP)Mn^{II}$ formed by controlled-potential electrolysis of $(Cl_8TPP)Mn^{III}Cl$ shows a characteristic Soret position at 436 nm. The third reduction (−1.70 V) of $(Cl_8TPP)Mn^{II}Cl$ {the one-electron reduction of $(Cl_8TPP^{\cdot-})Mn^{II}$} provides the visible spectrum ascribed to the dianion porphyrin of manganese $[(Cl_8TPP^{2-})Mn^{II}]$.

Reactivity of Manganese Tetra(2,6-dichlorophenyl) porphyrin with Hydroxide Ion. The reaction of $(Cl_8TPP)Mn^{III}Cl$ with hydroxide ion (TEAOH in H_2O) under an argon atmosphere has been investigated in MeCN or CH_2Cl_2 as solvents. Table 1 shows that the redox potentials of $(Cl_8TPP)Mn^{III}ClO_4$ are very similar to those of $(Cl_8TPP)Mn^{III}Cl$, and also the reaction of $(Cl_8TPP)Mn^{III}ClO_4$ with hydroxide ion (TEAOH in H_2O) are very similar to that of $(Cl_8TPP)Mn^{III}Cl$. Therefore, the results of $(Cl_8TPP)Mn^{III}Cl$ are explained in this study. The reactions have been monitored by UV-vis spectroscopy, where the spectral changes accompanying the reactions could be associated with changes in the oxidation and ligation states of $(Cl_8TPP)Mn^{III}Cl$. Figure 3 illustrates UV-vis spectra of 0.02 mM $(Cl_8TPP)Mn^{III}Cl$ (λ_{max} = 476 nm) and the reaction product [$A(\lambda_{max}$ = 444 nm)] of 0.02 mM $(Cl_8TPP)Mn^{III}Cl$ with excess (0.2 mM) hydroxide ion [$OH(H_2O)$] in MeCN.

In order to identify intermediates in the reaction of $(Cl_8TPP)Mn^{III}Cl$ with $OH(H_2O)$, the UV-vis spectral changes on addition of mole ratio of manganese porphyrin to hydroxide ion are studied in MeCN solutions. Figure 4 illustrates UV-vis spectra of reaction products obtained from the mole ratio (1 : 1) of 0.02 mM $(Cl_8TPP)Mn^{III}Cl$ to 0.02 mM hydroxide

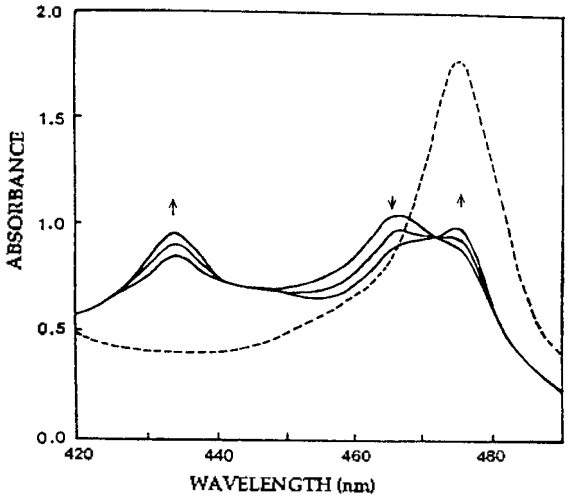

Figure 4. UV-vis absorption spectra of reaction products obtained from the mole ratio (1 : 1) of 0.02 mM $(Cl_8TPP)Mn^{III}Cl$ to 0.02 mM hydroxide ion [$OH(H_2O)$] in MeCN (spectral scans were taken at 60 sec intervals), and (dot line) a solution of $(Cl_8TPP)Mn^{III}Cl$.

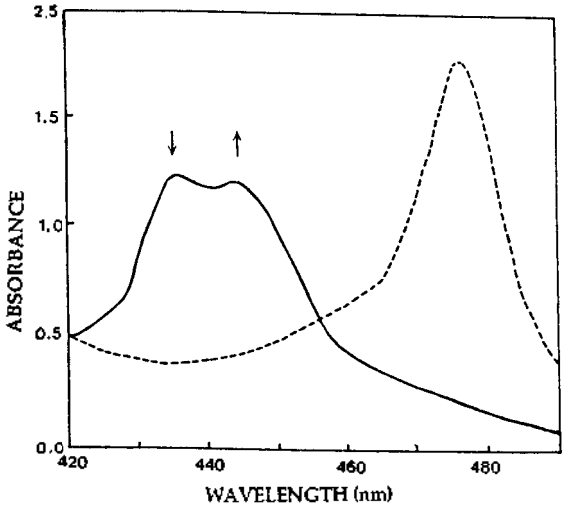

Figure 5. UV-vis absorption spectra of reaction products obtained from the mole ratio (1 : 2) of 0.02 mM $(Cl_8TPP)Mn^{III}Cl$ to 0.04 mM hydroxide ion [$OH(H_2O)$] in MeCN, and (dot line) a solution of $(Cl_8TPP)Mn^{III}Cl$.

ion [$OH(H_2O)$]. Figure 4 shows a decrease in the Soret position (λ_{max}=468 nm) of the initial product with concomitant increase in absorbances at both 436 and 476 nm. The initial product [**B**(λ_{max}=468 nm)] converts to a species (**C**) (λ_{max}=436 nm), and the starting compound $(Cl_8TPP)Mn^{III}Cl$ (λ_{max}=476 nm) is regenerated. There is seen isosbestic points (443, 472 nm) which demonstrates the absence of any long-lived intermediates.

Figure 5 shows visible spectra of reaction products obtained from the mole ratio (1 : 2) of 0.02 mM $(Cl_8TPP)Mn^{III}Cl$ to 0.04 mM hydroxide ion [$OH(H_2O)$] in MeCN. The reaction products are [**A** (λ_{max}=444 nm)] and a species [**C** (λ_{max}=436 nm)]. The arrows in Figure 5 indicate that the titration of an acetonitrile solution of $(Cl_8TPP)Mn^{III}Cl$ with aliquots of $OH(H_2O)$ gives the increase of a Soret absorbance at 444 nm with the decrease in absorbance at 436 nm. The titration of $(Cl_8TPP)Mn^{III}Cl$ with excess $OH(H_2O)$ only yields the reaction product [**A** (λ_{max}=444 nm)]. This result indicates that the reaction of $(Cl_8TPP)Mn^{III}Cl$ with $OH(H_2O)$ in MeCN makes initially $(Cl_8TPP)Mn^{II}$ (λ_{max}=436 nm), and then produces the adduct $\{[(Cl_8TPP)Mn^{II}(OH)]^-\}$ (λ_{max}=444 nm) obtained from $(Cl_8TPP)Mn^{II}$ and free $OH(H_2O)$ in MeCN. The reaction of $(Cl_8TPP)Mn^{III}Cl$ with excess $OH(H_2O)$ in the presence of pyridine or imidazole in MeCN as a ligating solvent also gives the oxidation state of manganese complexes [$(Cl_8TPP)Mn^{II}(py)$ or $[(Cl_8TPP)Mn^{II}(OH)]^-$].

On the basis of its Soret position, it can be concluded that the species (**A**) is assigned to $[(Cl_8TPP)Mn^{II}(OH)]^-$, because the Soret absorbance for the species (**A**) formed from the reaction of $(Cl_8TPP)Mn^{III}Cl$ with excess $OH(H_2O)$ is equivalent to that produced by the reaction of $(Cl_8TPP)Mn^{II}$ with $OH(H_2O)$. As different experiments, the titration of $(Cl_8TPP)Mn^{II}$ obtained electrochemically or chemically with excess $OH(H_2O)$ in MeCN produces the growth of a new Soret position at 444 nm with concomitant decrease in Soret absorbance at 436 nm of $(Cl_8TPP)Mn^{II}$. The species (**C**) of the absorbance at 436 nm is assigned to $(Cl_8TPP)Mn^{II}$ (probably coordinated by one MeCN), which is prepared independently through the electrochemical reduction of $(Cl_8TPP)Mn^{III}Cl$. The species (**B**) of the absorbance at 468 nm may be assigned to $(Cl_8TPP)Mn^{III}(OH)$ which is initially produced by the exchange of chloride ligand for hydoxide ion in the reaction of $(Cl_8TPP)Mn^{III}Cl$ with $OH(H_2O)$.

The spectrum change of $(Cl_8TPP)Mn^{III}Cl$ (λ_{max}=478 nm) in the presence of excess $OH(H_2O)$ in CH_2Cl_2 as a nonligating solvent only yields $[(Cl_8TPP)Mn^{III}(OH)]$ (λ_{max}=470 nm) by the exchange of chloride ligand for hydoxide ion. the spectrum of $(Cl_8TPP)Mn^{III}Cl$ (λ_{max}=478 nm) in CH_2Cl_2 is changed to $(Cl_8TPP)Mn^{III}Cl(MeCN)$ or $[(Cl_8TPP)Mn^{III}(MeCN)_2]^+$ (λ_{max}=476 nm) on addition of MeCN in CH_2Cl_2 or in MeCN solution. Meanwhile, in DMF or DMSO as other ligating solvents, the spectrum of $(Cl_8TPP)Mn^{III}Cl$ (λ_{max}=478 nm) in CH_2Cl_2 is changed to $[(Cl_8TPP)Mn^{III}(DMF)_2]^+$ (λ_{max}=466 nm) and $[(Cl_8TPP)Mn^{III}(DMSO)_2]^+$ (λ_{max}=464 nm) on addition of DMF or DMSO in CH_2Cl_2, respectively.

The reaction of $(Cl_8TPP)Mn^{III}Cl$ with excess $OH(H_2O)$ in the presence of MeCN or pyridine in CH_2Cl_2 yields $(Cl_8TPP)Mn^{III}(OH)$ (λ_{max}=468 nm) as the initial product, and slowly converts to $[(Cl_8TPP)Mn^{II}(OH)]^-$ (λ_{max}=444 nm). The reaction of $(Cl_8TPP)Mn^{III}Cl$ with excess $OH(H_2O)$ in pyridine as a ligating solvent yields the species $(Cl_8TPP)Mn^{II}(py)$ or $[(Cl_8TPP)Mn^{II}(OH)]^-$, because pyridine solvent seems effectively to trap hydroxy radical generated from the reaction of $(Cl_8TPP)Mn^{III}Cl$ with $OH(H_2O)$.[39]

Discussion

In nonligating solvents such as CH_2Cl_2, $(Cl_8TPP)Mn^{III}Cl$ does not dissociate and forms five-coordinate manganese(III) porphyrin.[40] However, in ligating solvents or when potential ligands are present, the six-coordinate Mn^{III} form is yielded by the ligation of solvent or potential ligand to manganese center. $(Cl_8TPP)Mn^{III}Cl$ could be present as $(Cl_8TPP)Mn^{III}Cl(MeCN)$ or $[(Cl_8TPP)Mn^{III}(MeCN)_2]^+$ in MeCN solution due

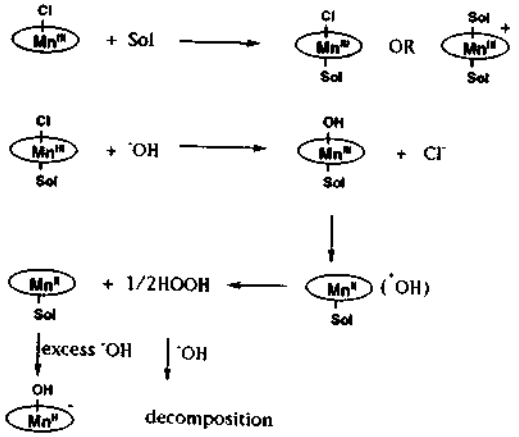

Scheme 1.

to the slightly blue shift of Soret position from 478 nm in CH_2Cl_2 as a solvent to 476 nm in the presence of MeCN in CH_2Cl_2 or in MeCN as a solvent.

The possible mechanism of $(Cl_8TPP)Mn^{III}Cl$ with $^-OH(H_2O)$ in MeCN as a ligating solvent may be summarized in terms of Scheme 1 (where Sol=ligating solvent, and the ellipses represent the porphyrin ring). The use of $^-OH(H_2O)$ excludes the existence of $^-OCH_3$ which may be generated from $^-OH(CH_3OH)$ used as a source of hydroxide ion in the previous studies.[35~36] Three intermediates, $(Cl_8TPP)Mn^{III}(OH)(Sol)$ (λ_{max}=476 nm), $(Cl_8TPP)Mn^{II}(Sol)$ (λ_{max}=436 nm) and $[(Cl_8TPP)Mn^{II}(OH)]^-$ (λ_{max}=444 nm), have been directly observed during the reaction. The favored products are five-coordinate rather than six-coordinate Mn^{II} forms, and six-coordinate Mn^{III} forms in ligating media. The autoreduction of $(Cl_8TPP)Mn^{III}Cl$ in the presence of $^-OH(H_2O)$ is dependent on the prior coordination of ligating solvents to $(Cl_8TPP)Mn^{III}Cl$ as an axial ligand. The role of the solvent as an axial ligand is explained by experiments in the nonligating solvent in the presence of MeCN or pyridine, where manganese(II) form is yielded.

The reduction of the initial intermediate $(Cl_8TPP)Mn^{III}(OH)(Sol)$ to form the manganese(II) porphyrin probably requires the electron transfer from ^-OH to manganese(III) within intramolecule. Possible mechanisms are discussed in the previous reports,[35] but they are still ambiguous. Mechanisms involve an inner sphere electron transfer from coordinated ^-OH to manganese(III) by homolytic Mn-O bond cleavage, or nucleophilic attack on coordinated ^-OH by free ^-OH. From UV-vis spectra of reaction products from the mole ratio (1 : 1) of $(Cl_8TPP)Mn^{III}Cl$ to $^-OH(H_2O)$ in MeCN that shows a decrease in the Soret position (λ_{max}=468 nm) of the initial product with accompanying increase in absorbances at both 436 and 476 nm, reasonable mechanism may be an inner sphere electron transfer from coordinated ^-OH to manganese(III) by homolytic Mn-O bond cleavage which would yield hydroxy radical(·OH) rather than a nucleophilic attack on coordinated ^-OH by free ^-OH.

The hydroxyl radicals that are yielded in the reaction could self-react to form hydrogen peroxide (HOOH). HOOH generated from the combination of hydroxy radicals reacts with free ^-OH or coordinated ^-OH to manganese(III) porphyrin to produce ^-OOH, which rapidly decomposes by the reaction with MeCN as a solvent.[41] Therefore, unfortunately free HOOH that are produced in the reaction of $(Cl_8TPP)Mn^{III}Cl$ and $^-OH(H_2O)$ can't be detected in MeCN solutions.

The electrochemical potential for the first reduction of $(Cl_8TPP)Mn^{III}Cl$ to give manganese(II) is −0.11 V, but −0.23 V for $(TPP)Mn^{III}Cl$ and −2.30 V for $(Me_{12}TPP)Mn^{III}Cl$. The positive potential for the reduction of $(Cl_8TPP)Mn^{III}Cl$ comes from the electronic effects of the substituted groups at *ortho*-position of phenyl group bonded to *meso*-position of porphyrin ring. This result indicates that $(Cl_8TPP)Mn^{III}Cl$ may be a stronger oxidizing agent than $(Me_{12}TPP)Mn^{III}Cl$ for the oxidation of hydroxide ion, and $(Cl_8TPP)Mn^{III}Cl$ easily reduces to manganese(II) by coordinated ^-OH (as a reducing agent) to core metal of manganese(III) porphyrin. It has reported that the oxidation potential for ^-OH in aprotic media shifts to negative upon addition of transition metal complexes.[26] This negative shift of oxidation potential for ^-OH is proposed to be due to the stabilization of hydroxyl radical by metal ion ligation *via* formation of a d-p covalent bond. The reaction of $(Me_{12}TPP)Mn^{III}Cl$ with excess $^-OH(CH_3OH)$ gives a species $[(Me_{12}TPP)Mn^{II}(OH)]^-$, which slowly oxidizes to $[(Me_{12}TPP)Mn^{III}(OH)_2]^-$.[35] However, in this study the reaction of $(Cl_8TPP)Mn^{III}Cl$ with excess $^-OH(H_2O)$ makes a species $[(Cl_8TPP)Mn^{II}(OH)]^-$, which is considerably stable and doesnot oxidize in the reaction solutions. The electrochemical and spectroscopic results estimate the importance of the axial ligands and the reduction potential of manganese porphyrins in determining the oxidation states of manganese porphyrins. The autoreduction of manganese(III) porphyrin to manganese(II) by this process is only observed when ^-OH can coordinate one axial site, and the other axial position occupied by a ligating solvent.

Acknowledgment. This research was supported in part by CNU Research Foundation (1995), in part by the basic science Research Institute program, Ministry of Education of Korea (BSRI 95-3429).

References

1. Hoffman, B. M.; Weschler, C. J.; Basolo, F. *J. Am. Chem. Soc.* **1978**, *100*, 4416.
2. Harriman, A. *J. Chem. Soc., Dalton Trans.* **1984**, 141.
3. Jin, T.; Suzuki, T.; Imamura, T.; Fujimoto, M. *Inorg. Chem.* **1987**, *26*, 1280.
4. *Cytochrome P-450: Structure, Mechanism and Biochemistry*; Ortiz de Montellano, P., Ed.; Plenum Press: New York, 1986.
5. Gunter, M. J.; Turner, P. *Coord. Chem. Rev.* **1991**, *108*, 115.
6. Renger, G. *Angew. Chem. Int. Ed. Engl.* **1987**, *26*, 643.
7. Dismukes, G. C. *Photochem. Photobiol.* **1986**, *43*, 99.
8. Michaelson, A. M.; McCord, J. M.; Fridovich, I. Eds *Superoxide and Superoxide Dismutases*; Academic Press: New York, 1977.
9. Pasternak, R. F.; Gibbs, E. J.; Villafranca, J. S. *Biochemistry* **1983**, *22*, 2406.
10. Ward, B.; Skorobogaty, A.; Dabrowiak, J. C. *Biochemistry* **1986**, *25*, 6875.
11. Rodriguez, M.; Kodadek, T.; Torres, M.; Bard, A. J. *Bio-*

conjugate Chem. **1990**, *1*, 123.
12. Yuan, L.-C.; Bruice, T. C. *J. Am. Chem. Soc.* **1986**, *108*, 1643.
13. Collman, J. P.; Brauman, J. I.; Meunier, B.; Hayashi, T.; Raybuck, S. A. *J. Am. Chem. Soc.* **1985**, *107*, 2000.
14. Groves, J. T.; Stern, M. K. *J. Am. Chem. Soc.* **1988**, *110*, 8628.
15. Brown, R. B., Jr.; Williamson, M. W.; Hill, C. L. *Inorg. Chem.* **1987**, *26*, 1602.
16. Creager, S. E.; Raybuck, S. A.; Murray, R. W. *J. Am. Chem. Soc.* **1986**, *108*, 4225.
17. Mu, X. H.; Schultz, F. A. *Inorg. Chem.* **1995**, *34*, 3835.
18. Mu, X. H.; Schultz, F. A. *Inorg. Chem.* **1992**, *31*, 3351.
19. Foran, G. J.; Armstrong, R. S.; Crossley, M. J.; Lay, P. A. *Inorg. Chem.* **1992**, *31*, 1463.
20. Hill, C. L.; Williamson, M. W. *Inorg. Chem.* **1985**, *24*, 2836.
21. Robert, A.; Loock, B.; Momenteau, M.; Meunier, B. *Inorg. Chem.* **1991**, *30*, 706.
22. Okumura, T.; Endo, S.; Ui, A.; Itoh, K. *Inorg. Chem.* **1992**, *31*, 1580.
23. Kadish, K. M.; Kelly, S. *Inorg. Chem.* **1979**, *18*, 2968.
24. Jones, D. H.; Hinman, A. S. *J. Chem. Soc., Dalton Trans.* **1992**, 1503.
25. Richert, S. A.; Tsang, P. K. S.; Sawyer, D. T. *Inorg. Chem.* **1989**, *28*, 2471.
26. Tsang, P. K. S.; Cofre, P.; Sawyer, D. T. *Inorg. Chem.* **1987**, *26*, 3604.
27. Mu, X. H.; Schultz, F. A. *J. Electroanal. Chem.* **1993**, *353*, 349.
28. Kelly, S.; Lancon, D.; Kadish, K. M. *Inorg. Chem.* **1984**, *23*, 1451.
29. Bettelheim, A.; Ozer, D.; Weinraub, D. *J. Chem. Soc., Dalton Trans.* **1986**, 2297.
30. Kelly, S.; Kadish, K. M. *Inorg. Chem.* **1982**, *21*, 3631.
31. Iwaizumi, M.; Komuro, H. *Inorg. Chim. Acta* **1986**, *111*, L9.
32. Kadish, K. M.; Morrison, M. M. *BioInorg. Chem.* **1977**, *7*, 107.
33. Livorness, J.; Smith, T. D. *Struct. Bonding* **1982**, *48*, 1.
34. Kok, B.; Forbush, B.; McGloin, M. *Photochem. Photobiol.* **1970**, *11*, 457.
35. Arasasingham, R. D.; Bruice, T. C. *Inorg. Chem.* **1990**, *29*, 1422.
36. Nakagaki, P. C.; Calderwood, T. S. Bruice, T. C. *Proc. Natl. Acad. Sci. USA* **1988**, *85*, 5424.
37. Wagner, R. W.; Lawrence, D. S.; Lindsey, J. S. *Tetrahedron Lett.* **1987**, *28*, 3069.
38. Lindsey, J. S.; Wagner, R. W. *J. Org. Chem.* **1989**, *54*, 828.
39. Srivatsa, G. S.; Sawyer, D. T. *Inorg. Chem.* **1985**, *24*, 1732.
40. Boucher, L. J. *Coord. Chem. Rev.* **1972**, *7*, 289.
41. Sawyer, D. T. *Oxygen Chemistry, Chap. 8*; Oxford University Press: London, 1991.

The SCF and CI Study on Vibrational Structures of Triatomic van der Waals Complexes: He-I_2 and He-Cl_2

Jeong'hee Seong and Hosung Sun*

Department of Chemistry, Pusan National University, Pusan 609-735 and Center for Molecular Science, KAIST, Taejon 305-701, Korea

Received July 30, 1996

The vibartional energy levels of triatomic van der Waals complexes, *e.g.*, He-I_2 and He-Cl_2, are studied theoretically. Not only because a weak bond exists in these systems but also because the excited states are of interest, very accurate numerical methods are required to determine vibrational structures of the complexes. The self-consistent-field (SCF) and the configuration interaction (CI) methods are employed to study several low lying bound states. Particularly the useful but approximate SCF method is extensively studied by comparing its results with those of in-principle-accurate CI method. It is found that the SCF method produces reasonable vibrational energy levels when Jacobi coordinates are utilized.

Introduction

The van der Waals complexes, *i.e.*, molecules having at least one chemically weak van der Waals bond, have attracted a lot of attention both experimentally and theoretically.[1~22] Experimental techniques such as high-resolution IR absorption spectroscopy, Fourier-transform infrared spectroscopy, and microwave spectroscopy provide a wealth of information on the geometrical and vibrational structures of van der Waals complexes. In many weakly bound molecules the deviation from harmonic behavior is very large even for ground vibrational state. It is to obtain the vibrational energy level structure of the complexes from the given potential energy functions and to interpret the level structure in terms of vibrational dynamics involved. The need for theoretical methods arises from the very rapid progress in experimental